
MAD@VLT: Deep into the Madding Crowd of Omega Centauri

G. Bono^{1,2}, A. Calamida¹, C. E. Corsi¹, P.B. Stetson³, E. Marchetti², P. Amico², P.G. Prada Moroni⁴, I. Ferraro¹, G. Iannicola¹, M. Monelli⁵, R. Buonanno⁶, F. Caputo¹, M. Dall’Ora⁷, S. Degl’Innocenti⁴, S. D’Odorico², L. M. Freyhammer⁸, D. Koester⁹, M. Nonino¹⁰, A.M. Piersimoni¹¹, L. Pulone¹, and M. Romaniello²

¹ INAF-OAR, via Frascati 33, 00040 Monte Porzio, Italy bono@mporzio.astro.it

² ESO, Karl-Schwarzschild-Str. 2, 85748 Garching bei Munchen, Germany

³ DAO, HIA-NRC, 5071 West Saanich Road, Victoria BC V9E 2E7, Canada

⁴ INFN, Sez. Pisa, via Largo B. Pontecorvo 2, 56127 Pisa, Italy

⁵ IAC, Calle Via Lactea, E38200 La Laguna, Tenerife, Spain

⁶ Univ. di Roma Tor Vergata, via della Ricerca Scientifica 1, 00133 Rome, Italy

⁷ INAF-OAC, via Moiarriello 16, 80131 Napoli, Italy

⁸ Centre for Astrophysics, University of Central Lancashire, Preston PR1 2HE

⁹ Institut Theoretische Physik & Astrophysik, Univ. of Kiel, 24098 Kiel, Germany

¹⁰ INAF-OAT, via G.B. Tiepolo 11, 40131 Trieste, Italy

¹¹ INAF-OACT, via M. Maggini, 64100 Teramo, Italy

1 Abstract

We present deep and accurate Near-Infrared (NIR) photometry of the Galactic Globular Cluster (GC) ω Cen. Data were collected using the Multi-Conjugate Adaptive Optics Demonstrator (MAD) on VLT (ESO). The unprecedented quality of the images provided the opportunity to perform accurate photometry in the central crowded regions. Preliminary results indicate that the spread in age among the different stellar populations in ω Cen is limited.

2 Introduction

Quantitative constraints concerning the evolutionary properties of low-mass stars mainly rely on the comparison between predicted and observed Color-Magnitude Diagrams (CMDs) of GCs. The GCs present several key advantages when compared with field stars: *i*) cluster stars typically present the same age and the same chemical composition; *ii*) cluster stars are located at the same distance, since the depth effects are negligible, and present the same reddening; *iii*) cluster stars in a CMD are distributed according to their

evolutionary status, (*consecutio*), therefore, they are redundant systems; *iv*) cluster cores host a zoo of compact objects: Cataclysmic Variables (Edmonds et al. 2003), Millisecond pulsars (Freire et al. 2003), Low-Mass X-ray Binaries (Heinke et al. 2005) and probably either a low or intermediate-mass black hole (Bash et al. 2008).

The main drawback of GCs is that quite often more than half of the cluster stars are located in the innermost regions, and indeed the half mass radius of massive clusters is at most a few arcminutes. This is the reason why accurate and deep photometry of the innermost regions of GCs became chore only with the superb spatial resolution and image quality of the Hubble Space Telescope (HST) optical images. It is worth mentioning that accurate photometry in the crowded central regions of GCs is not a trivial effort even by using HST images.

Among the Galactic GCs, ω Cen appears to be a peculiar system. It is the only one to show a well defined spread in the abundance of iron and α -elements, thus suggesting that it might be a possible link between GCs and dwarf galaxies. It is also the most massive GC. This means that ω Cen is a perfect laboratory to investigate fast evolutionary phases (Calamida et al. 2008) and to constrain the chemical enrichment from supernovae ejecta and from previous generations of intermediate-mass AGB stars. The use of optical and NIR photometry of cluster stars presents several advantages when compared with either optical or NIR photometry. The stronger temperature sensitivity of optical-NIR colors provides the opportunity to select candidate cluster and field stars (Calamida et al. 2007). For the same reasons, the optical-NIR colors can be adopted to pinpoint peculiar stellar populations that present either different ages or different chemical compositions (Freyhammer et al. 2005).

3 Observations and Data Reduction

Optical data were collected with the Advanced Camera for Surveys (ACS) on board the HST and the reduction strategy was already discussed by Castellani et al. (2007) and by Calamida et al. (2008).

MAD is a prototype instrument performing wide Field of View (FoV) real-time correction for atmospheric turbulence (Marchetti et al. 2006). MAD has been built by ESO with the contribution of two external consortia to prove on the sky the feasibility of Multi-Conjugate Adaptive Optics (MCAO) technique in the framework of the 2nd generation VLT instrumentation and of the European Extremely Large Telescope (Gilmozzi & Spyromilio 2007). The key advantage of MCAO is to increase the size of the FoV corrected for atmospheric turbulence. The principle of MCAO is based on probing the volume of atmospheric turbulence above the telescope by performing wavefront sensing on several guide stars in the FoV. This goal is reached by implementing a tomographic reconstruction of the turbulence (Ragazzoni, Marchetti & Valente 2000) to constrain its 3D distribution and then by applying the correction

using several deformable mirrors optically conjugated at different altitudes in the atmosphere.

MAD is equipped with three Shack-Hartmann wavefront sensors for measuring the atmospheric turbulence from three guide stars located in a FoV of 2 arcminutes. Depending on the atmospheric seeing conditions the limiting magnitude for the guide stars can be up to $V \sim 13$. CAMCAO is the MAD NIR camera and it is based on a 2048x2048 pixels Hawaii2 infrared detector with a pixel scale of 0.028 arcsec per pixel for a total FoV of 57.3 arcsec. CAMCAO is mounted on a movable table to scan the full 2 arcminutes FoV. The camera is equipped with a standard set of J , H and K_s filters. MAD has been installed at the Visitor Focus of the VLT telescope UT3 (Melipal) located at the ESO Paranal Observatory.

During the first on-sky demonstration run of MAD two 1x1 arcminute fields were observed in the region across the center of ω Cen. The first field was centered at RA=201.66, DEC=-47.46 and it was observed on April 3rd, 2007. For wavefront sensing we used three guide stars of magnitude $V \sim 11.5$ and the MCAO loop was closed at a correction frequency of 400 Hz. Five images of 5×24 sec each were collected in K_s -band and three images of 5×24 sec each in J -band. The second field is centered at RA=201.64, DEC=-47.45 and it was observed on April 4th, 2007. For wavefront sensing we used three guide stars of magnitude $V \sim 11.5$ equally distributed on a circle of 1 arcmin diameter concentric to the field and the MCAO loop was closed at a correction frequency of 400 Hz. Four images of 10×24 sec were collected in K_s -band and three images of 10×24 sec in J -band. The seeing during the observations of the first night changed from 0.7 to 0.9 arcsec, while during the second it changed from 0.9 to 1.2 arcsec.

The photometry was performed using DAOPHOTIV/ALLSTAR and ALLFRAME (Stetson 1994). We selected ≈ 100 isolated stars to estimate an analytical point-spread function (PSF) for each frame. We adopted a Moffat function with $\beta = 2.5$ for the PSF of the K_s -band images with a quadratic positional change. For the J -band images we adopted for the PSF either a Moffat, with $\beta = 1.5$, or a Lorentz function, and they were assumed linearly variable across the chip. We performed PSF analytical photometry on individual NIR images with ALLSTAR.

Then NIR and optical images were simultaneously reduced using ALLFRAME and the final catalog includes $\approx 7.5 \times 10^5$ stars. The comparison between the optical and NIR catalogs indicates that on MAD images we identified on average more than 90% (K_s -band) and more than 75% (J -band) of the stars detected in the same cluster regions using ACS images. The photometric calibration of NIR data into the 2MASS system was performed using a sample of ~ 5000 local standard stars (Del Principe et al. 2006). The accuracy of the absolute zero-point calibration is ~ 0.02 mag for the K_s -band and ~ 0.03 mag for the J -band. We ended up with an optical-NIR catalog including $\approx 49,000$ (K_s) and $\approx 41,000$ (J) stars with at least one measurement in an optical and in a NIR band.

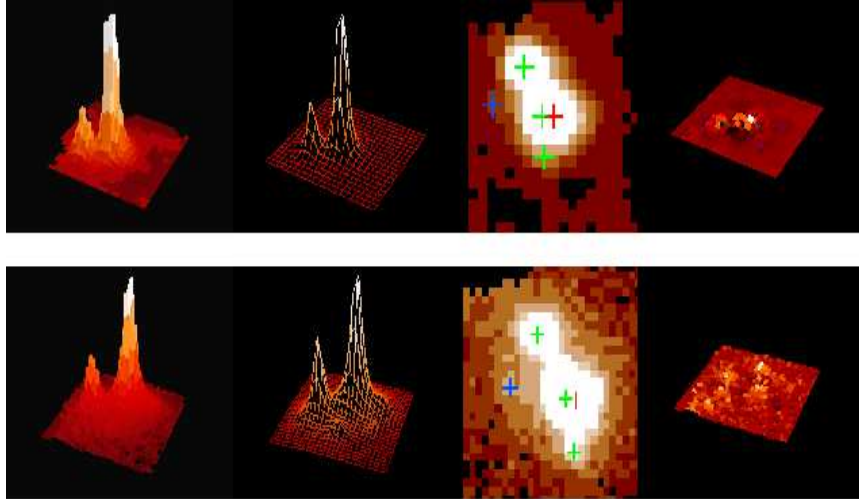


Fig. 1. Top – from left to right: the 3D shape of a group of five MS stars in a $F435W$ ACS image of 340 sec. Analytical Moffat PSF model of the stars plotted in the left panel. Top view of the same stars. The red plus marks the brightest star, while the blue plus the star that was identified in the MAD image. Residuals after the subtraction of the analytical PSF to the data. Bottom – Same as the top panels, but in a K_s MAD image of 120 sec. Note the difference in spatial resolution of optical and NIR images and the smooth distribution of the residuals.

The images plotted in the upper panels of Fig. 1 show a group of five Main Sequence (MS) stars in a $F435W$ -band ACS image. The exposure time of this image is 340 sec and it is located across the cluster center. The brightest object in the group is located a couple of magnitudes below the Turn-Off (TO) region ($F435W \sim 19.9$), while the faintest is almost two orders of magnitude fainter ($F435W \sim 24.5$). The lower panels show the same group of stars but in a K_s -band MAD image. The exposure time of this image is 120 sec. The stars quoted above present K_s magnitudes of ~ 16.9 and ~ 19.4 mag, respectively. The full-width-half-maximum (FWHM) of MAD images is typically better than 0.1 arcsec in the K_s -band and better than 0.25 arcsec in the J -band. This together with the good spatial resolution and image quality provided the opportunity to perform accurate ground-based PSF photometry in crowded cluster regions. The residuals of the fits (rightmost panels) are smaller than 1% both in the optical and in the NIR images. In passing, we note that the faintest star (blue plus) was firstly detected in the MAD images and then added in the fit of the ACS images.

The NIR bands present several advantages when compared with the optical bands. *i)* They are marginally affected by reddening uncertainties and by the possible occurrence of differential reddening (Calamida et al. 2005; van Loon et al. 2007). *ii)* When moving from MSTO stars down to very-low-mass stars

the range of NIR magnitudes covered by these structures is quite limited $17 \leq K_s \leq 21$. On the other hand, the same structures in the $F435W$ and in the $F625W$ band cover 8 and 7 mag, respectively. The difference is due to the fact that less massive MS structures are also steadily cooler, therefore, their emissivity peaks in the NIR bands.

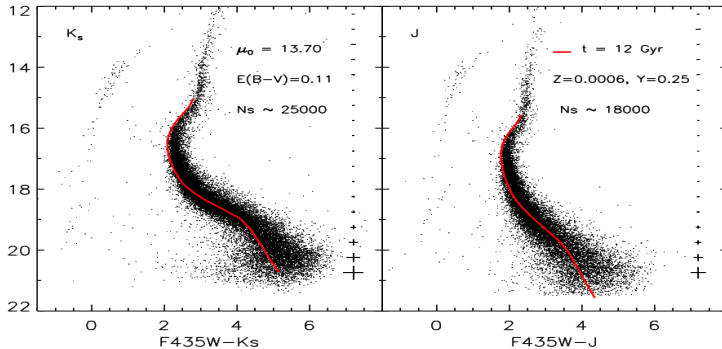


Fig. 2. Left – K_s vs $F435W - K_s$ CMD of ω Cen based on data collected with MAD@VLT and with ACS@HST. Current data extend from hot HB stars $K_s \sim 13.5$, $F435W - K_s \sim 1.0$ down to the regime of very-low-mass stars $K_s \sim 21$, $F435W - K_s \sim 6.0$. By assuming $\mu = 13.70$, $E(B - V) = 0.11$ and evolutionary prescriptions by Castellani et al. (2007), in this region of the MS are located structures with a stellar mass $M \approx 0.3M_\odot$. Right – same as the left, but for the J vs $F435W - J$ CMD of ω Cen.

Data plotted in Fig. 2 show the optical-NIR ($K_s, F435W - K_s$; $J, F435W - J$) CMDs of ω Cen based on MAD and ACS images. To our knowledge this is the deepest $K_s, F435W - K_s$ CMD ever collected for a GC. The fit with a cluster isochrone of 12 Gyr (red line) indicates that we detected MS stars with mass values $M \leq 0.3M_\odot$ ($K_s \approx 21$, left panel). The J -band photometry reaches similar limiting magnitudes, but the CMD is slightly shallower. In passing, we note that current photometry suggests that the age spread in ω Cen appears to be limited, and indeed the color age derivative at fixed metal content ($Z = 0.0006$) is $\Delta(F435W - K_s)/\Delta age \sim 0.06$ mag/Gyr.

In order to constrain the impact that MAD has on the photometry of crowded regions, Fig. 3 shows the optical-NIR CMD based on data of the same cluster regions collected with SOFI@NTT and with ISAAC@VLT. The exposure time of the NIR images is 240 (K_s) and 180 (J) sec for SOFI and 78 (K_s) and 66 (J) sec for ISAAC. The observing strategy we adopted to reduce these data is very similar to the approach discussed in §2. The NIR limiting magnitudes of this data set is $\approx 3-4$ mag brighter than the MAD data set. The difference in the two data sets is mainly due to different seeing conditions: 0.5–0.7 arcsec (K_s, J ; SOFI), 0.4–0.6 arcsec (K_s, J ; ISAAC) versus 0.1–0.2 arcsec for MAD. An important role is also played by the spatial resolution ~ 0.29

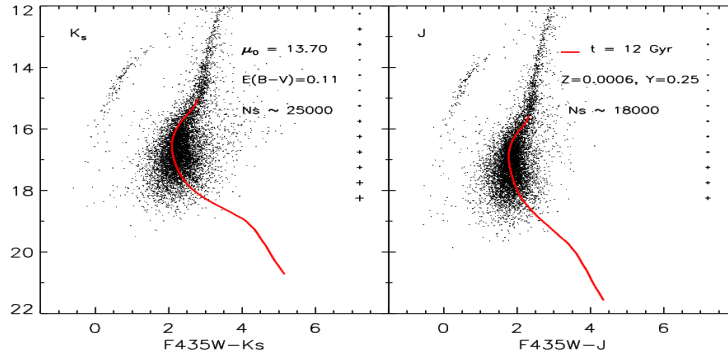


Fig. 3. Same as Fig. 2, but NIR data collected with SOFI@NTT and ISAAC@VLT.

arcsec/px (SOFI), ~ 0.15 arcsec/px (ISAAC) versus ~ 0.03 arcsec/px (MAD). This has a twofold impact on the intrinsic accuracy of PSF photometry: *i*) the improvement in the sampling implies a more accurate image deblending; *ii*) the decrease in the pixel scale also implies smaller fluctuations in the sky background, and in turn, a more efficient identification of fainter sources.

Preliminary results based on NIR data of ω Cen collected with MAD@VLT appear very promising in performing accurate and deep photometry in the innermost crowded regions of GCs. Up to now these regions have only been investigated using HST. Current Adaptive Optics systems have been developed for NIR bands. The use of these bands presents several advantages in constraining the evolutionary properties of very-low-mass stars and the cooling sequence of cluster white dwarfs (Calamida et al. 2008, in preparation).

References

1. A. Calamida, et al.: ApJ **634**, L69 (2005)
2. A. Calamida, et al.: ApJ **670**, 400 (2007)
3. A. Calamida, et al.: ApJ **673**, L29 (2008)
4. V. Castellani, A. Calamida, G. Bono, et al.: ApJ **663**, 1021 (2007)
5. M. Del Principe, et al.: ApJ **652**, 362 (2006)
6. R. Gilmozzi, J. Spyromilio: Msngr **127**, 11 (2007)
7. L.M. Freyhammer, et al.: ApJ **623**, 860 (2005)
8. E. Marchetti, R. Brast, B. Delabre, et al.: MAD star oriented: laboratory results for ground layer and multi-conjugate adaptive optics, SPIE **6272**, 21 (2006)
9. R. Ragazzoni, E. Marchetti, G. Valente: Nature **403**, 54 (2000)
10. P.B. Stetson: PASP, **106**, 250 (1994)
11. J.Th. van Loon: MNRAS, **382**, 1353 (2007)